

minutes to hours) to the kinetic and thermodynamic properties of single polymers; investigation of folding/unfolding in physiological ionic strengths and temperatures; and determination of the effects of ions, drugs, and proteins on RNA structure (27).

References and Notes

1. X. Zhuang et al., *Science* **288**, 2048 (2000).
2. J. H. Cate et al., *Science* **273**, 1678 (1996).
3. J. H. Cate, R. L. Hanna, J. A. Doudna, *Nature Struct. Biol.* **4**, 553 (1997).
4. D. K. Treiber, J. R. Williamson, *Curr. Opin. Struct. Biol.* **9**, 339 (1999).
5. A. R. Ferre-D'Amare, J. A. Doudna, *Annu. Rev. Biophys. Biomol. Struct.* **28**, 57 (1999).
6. A. M. Pyle, *Science* **261**, 709 (1993).
7. M. Wu, I. Tinoco Jr., *Proc. Natl. Acad. Sci. U.S.A.* **95**, 11555 (1998).
8. C. Y. Ralston, Q. He, M. Brenowitz, M. R. Chance, *Nature Struct. Biol.* **7**, 371 (2000).
9. J. Pan, D. Thirumalai, S. A. Woodson, *Proc. Natl. Acad. Sci. U.S.A.* **96**, 6149 (1999).
10. The DNA-RNA hybrid molecules were prepared by annealing the ends of a ~1.2-kb RNA to complemen-

tary DNA molecules (12). Pulling experiments were performed at 298 K in 10 mM Tris, 250 mM NaCl, and either 10 mM MgCl₂ or EDTA.

11. S. B. Smith, Y. Cui, C. Bustamante, *Science* **271**, 795 (1996).
12. Supplementary material is available on Science Online at www.sciencemag.org/cgi/content/full/292/5517/733/DC1.
13. B. Essevaz-Roulet, U. Bockelmann, F. Heslot, *Proc. Natl. Acad. Sci. U.S.A.* **94**, 11935 (1997).
14. M. Reif, H. Clausen-Schaumann, H. Gaub, *Nature Struct. Biol.* **6**, 346 (1999).
15. Unless indicated otherwise, free energies are valid for a force of $F_{1/2}$, 298 K, and 250 mM NaCl, 10 mM Mg²⁺.
16. M. Zuker, *Curr. Opin. Struct. Biol.* **10**, 303 (2000).
17. J. G. Kirkwood, I. Oppenheim, *Chemical Thermodynamics* (McGraw-Hill, New York, 1961).
18. $\Delta x(F_{1/2}) = \Delta x_{1/2}$ was obtained from plots of $\ln K_{eq}(F)$ versus force using $d \ln K_{eq}(F)/dF = \Delta x(F)/k_B T$, where $\Delta x(F)$ was expanded as $\Delta x_{1/2} + (F - F_{1/2})dx/dF$. The WLC model gives (high-force limit) $dx/dF = L(4F\sqrt{FP/k_B T})^{-1}$.
19. The measured rate constants are the rates with which the entire system (beads, handles, and RNA) hops from one extension to another. The various contributions are expressed in Eq. 1 as the product of a

"machine" constant k_m and a molecule constant k_0 . Therefore, hopping reveals the sensitivity of RNA folding/unfolding to external force (the distance to the transition state Δx^\ddagger) and the difference between the ΔG^\ddagger values (the ΔG of unfolding), but not the absolute rates or ΔG^\ddagger values (12).

20. E. Evans, K. Ritchie, *Biophys. J.* **72**, 1541 (1997).
21. M. Carrion-Vazquez et al., *Proc. Natl. Acad. Sci. U.S.A.* **96**, 3694 (1999).
22. M. S. Kellermayer, S. B. Smith, H. L. Granzier, C. Bustamante, *Science* **276**, 1112 (1997).
23. C. Ma, V. A. Bloomfield, *Biopolymers* **35**, 211 (1995).
24. V. K. Misra, D. E. Draper, *Biopolymers* **48**, 113 (1998).
25. U. Bockelmann, B. Essevaz-Roulet, F. Heslot, *Phys. Rev. E* **58**, 2386 (1998).
26. I. Tinoco Jr., C. Bustamante, *J. Mol. Biol.* **293**, 271 (1999).
27. This research was supported in part by NIH grants GM-10840 and GM-32543, Department of Energy grants DE-FG03-86ER60406 and DE-AC03-76SF00098, and NSF grants MBC-9118482 and DBI-9732140. J.T.L. is supported by the Program in Mathematics and Molecular Biology through a Burroughs Wellcome Fund Fellowship.

20 December 2000; accepted 13 March 2001

Switching Repulsion to Attraction: Changing Responses to Slit During Transition in Mesoderm Migration

Sunita G. Kramer, Thomas Kidd,* Julie H. Simpson, Corey S. Goodman†

Slit is secreted by cells at the midline of the central nervous system, where it binds to Roundabout (Robo) receptors and functions as a potent repellent. We found that migrating mesodermal cells in vivo respond to Slit as both an attractant and a repellent and that Robo receptors are required for both functions. Mesoderm cells expressing Robo receptors initially migrate away from Slit at the midline. A few hours after migration, these same cells change their behavior and require Robo to extend toward Slit-expressing muscle attachment sites. Thus, Slit functions as a chemoattractant to provide specificity for muscle patterning.

Migrating cells are guided by attractive and repulsive signals (1). Many of these factors are bifunctional (1–5). In addition, migrating cells can switch on or off their responsiveness to particular guidance cues (6–8). In vitro, growth cones can switch between attraction and repulsion if the internal state of the cell is altered [e.g., (9, 10)]. Here we show that such a change takes place in the developing mesoderm in the *Drosophila* embryo. Migrating mesodermal cells switch their responsiveness to Slit as they switch phases in their differentiation. Initially, they are repelled by Slit

emanating from the midline, but only a few hours later, they are attracted to Slit secreted by epidermal muscle attachment sites (MASs).

The first phase of cell migration during *Drosophila* myogenesis occurs after gastrulation, when muscle precursor cells migrate through the ventral furrow and spread dorsally to coat the inner surface of the ectoderm. In the second phase, muscle precursors fuse to form individual muscle fibers as they extend growth cone-like processes, which migrate toward specific MASs within the epidermis (11–13).

The migration of the mesodermal cells that will form ventral muscles is dependent on the expression of Slit, an extracellular matrix molecule secreted by midline cells (14). In *slit* mutant embryos, many ventral muscle precursors fail to migrate away from the midline and fuse to form muscles that

inappropriately stretch across the central nervous system (CNS) (Fig. 1B) (15, 16). On the basis of staining with several muscle-specific markers, we identified most of these misplaced muscles as ventral muscles 6 and 7 (17). These defects are rescued by expressing *UAS-slit* at the ventral midline using *single-minded-GAL4* (18), confirming that the midline expression of Slit is required for the migration of muscle precursors away from this region (Fig. 1D) (16).

In the *Drosophila* CNS, Slit is the repulsive ligand for the Roundabout (Robo) family of receptors (7, 15, 19–23). The *Drosophila* genome encodes three Robo receptors: Robo, Robo2, and Robo3. Robo and Robo2 together control repulsive axon guidance at the midline (20, 22). The repulsion of mesodermal cells by Slit at the midline also requires Robo and Robo2. In *robo* mutant embryos, occasional muscles can be seen crossing the midline (15, 16), whereas in the *robo, robo2* double mutant, the muscle phenotype resembles that of *slit*, with most segments containing multiple muscles 6 and 7 stretched across the midline (Fig. 1C) (16). This defect can be rescued by expressing either a *robo* or *robo2* transgene in all muscles with the *24B-GAL4* driver (18).

After their migration away from the midline, specific muscle precursor cells fuse with neighboring myoblasts to form muscle fibers (11, 24). These muscles extend growth cone-like processes toward their appropriate MASs (12, 13). Little is known about the cues that guide these cell-specific migrations. Here we show that Slit is one of these cues, but in this case, Slit functions as an attractant for muscles expressing Robo and/or Robo2.

All MASs express the zinc-finger protein Stripe (Fig. 2A) (18, 25). Beginning at stage 13 of embryogenesis, *slit* is also expressed at the subset of MASs that lies along the segment

Howard Hughes Medical Institute, Department of Molecular and Cell Biology, 519 Life Sciences Addition, University of California, Berkeley, CA 94720, USA.

*Present address: Exelixis, 170 Harbor Way, Post Office Box 511, South San Francisco, CA 94083–0511, USA.

†To whom correspondence should be addressed.

borders where longitudinal muscles (and certain other oblique muscles) attach (Fig. 2C). Slit is absent from MASs for lateral transverse muscles 21 through 24, which attach away from the segment borders. The expression of Slit at a subset of MASs suggests a role for Slit in muscle attachment specificity. Moreover, it suggests that the function of Slit in muscle development is not exclusively repulsive.

Robo and Robo2 are expressed at the sites of contact between the longitudinal muscles and their Slit-positive MASs (Fig. 2B). Furthermore, the two receptors are absent in those transverse muscles that extend toward Slit-negative MASs.

We used confocal microscopy to confirm the cellular localization of Slit and Robo along with D-MEF2, a transcription factor that stains muscle cells (26). Slit is localized to the outer epidermal cell layer and is concentrated at the MASs (Fig. 2D). Robo localizes to the muscle cell layer, with the protein concentrated at the ends of the muscles where they make contact with the Slit-expressing epidermis (Fig. 2E).

If Slit plays a role in guiding muscle pioneers toward their correct MASs, then we would expect muscle patterning defects in *slit* mutant embryos, distinct from those due to its initial role as a midline repellent. To test this, we rescued *slit* mutant embryos by driving *UAS-slit* with *single-minded-GAL4*. In these embryos, the initial migration defect seen in the ventral muscle precursors is rescued (Fig. 1D). However, striking defects are seen during the second phase, as muscles extend toward their MASs. Many muscles that normally attach at Slit-positive MASs are instead attached to the wrong sites in the epidermis (Figs. 3C and 4). We found no substantial defects in Stripe expression, indicating that these defects are not due to a loss of MASs (27). These results suggest that Slit at MASs acts as a chemoattractant to guide migrating muscle cells.

Muscles 6 and 7 are among the muscles that have attachment defects. These muscles normally stretch between segment borders and make connections at Slit-positive MASs (Figs. 3B and 4A). In *slit* (midline-rescued) mutants, these muscles often do not reach their MASs, or they make abnormal connections with the epidermis (Figs. 3C and 4B) (16). Thus, in the initial phase of mesoderm migration, the precursors for muscles 6 and 7 were repelled by the Slit-positive midline (Fig. 1, B and C) (17), but now a few hours later, these cells are attracted to Slit-positive MASs.

Muscle 5 also has attachment defects in *slit* mutants. This muscle attaches at two sites along the segment borders that are Slit-positive (Figs. 3B and 4C). In *slit* (midline-rescued) mutants, this muscle is often missing or not properly attached at one or both ends (Figs. 3C and 4D) (16). This defect is not due to a loss in the muscle 5 precursor (18, 28). Therefore, precursor

cell identity appears not to be altered in *slit* embryos. Rather, the migrating muscle fiber is guided to the wrong place.

To test whether Slit is signaling through Robo receptors in this pathway, we tested for genetic interactions between Slit and Robo. In either *slit,robo* or *slit,robo2* transheterozygotes, we seldom observe muscle insertion defects. However, in embryos that are transheterozygous for all three genes, we observe frequent defects in muscle attachment, similar to the defects seen in a midline-rescued *slit* homozygous mutant (16). For example, muscle 5 is often misinserted. Together with the expression data, these results suggest that Slit functions through Robo receptors to attract a specific class of migrating muscle cells to their appropriate MASs.

Muscles 21 through 23 normally do not express high levels of Robo or Robo2. Likewise, Slit protein is not detected at their MASs (Figs. 2 and 3). The correct migration of these muscles requires the expression of *derailed* (*drl*), a receptor tyrosine kinase, also involved in midline axon guidance. In *drl* mutants, muscles 21 through 23 frequently bypass their normal MASs and continue to extend ventrally (29). As predicted, these muscles are not severely altered in *slit* mutants (30). If Slit is indeed a chemoattractant for muscles expressing Robo, then ectopically expressing Robo in these muscles might cause them to be attracted to Slit-positive MASs. To test this hypothesis, we expressed Robo or Robo2 in all muscles using the *24B-GAL4* line (31). In these flies, muscles 21 through 23, which now abnormally express Robo or Robo2, turn and make attachments at

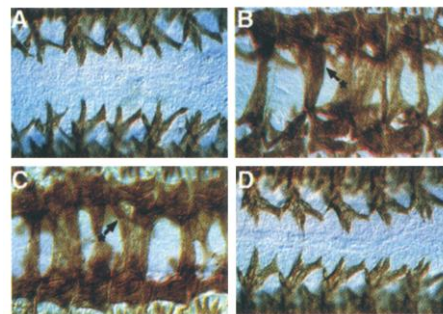


Fig. 1. Slit, Robo, and Robo2 are required for the repulsion of mesoderm cells away from the ventral midline, as shown by stage 16 embryos stained with an antibody to muscle myosin. Anterior is to the left and the ventral midline is the horizontal middle of each panel. (A) Wild-type embryo. The ventral muscles are arranged in a segmental pattern on either side of the midline and anchor to the epidermis underneath the CNS (above the plane of focus). (B) *slit* embryo. The ventral muscles fail to migrate away from the midline, resulting in muscles that extend over the dorsal surface of the CNS. Arrow with * indicates ventral longitudinal muscles 6 and 7. (C) The *robo,robo2* double mutant is largely identical to *slit*. (D) The *slit* phenotype is rescued by driving *UAS-slit* with *single-minded-GAL4* (18).

the segment borders (Figs. 3E and 4E) toward Slit-positive MASs (Fig. 2C). These muscles are no longer attracted to these sites in a *slit* mutant, confirming that these muscles were indeed attracted to Slit (Fig. 4F).

The experiments described thus far show that Slit at MASs is an attractant for migrating mesoderm cells. Does this require only Slit, or does some other cue at the MASs help convert Slit responsiveness from repulsion to attraction? To distinguish between these two possibilities, we ectopically expressed Slit at different locations in the epidermis. We crossed *UAS-slit* flies to the *engrailed-GAL4* or *patched-GAL4* lines (18). *engrailed-GAL4* drives expression in a segmental pattern that only partially overlaps the MAS cells. *patched-GAL4* expresses in a broad epidermal stripe in the center of each segment. When *slit* is expressed by these GAL4 lines in wild-type embryos, we observe little

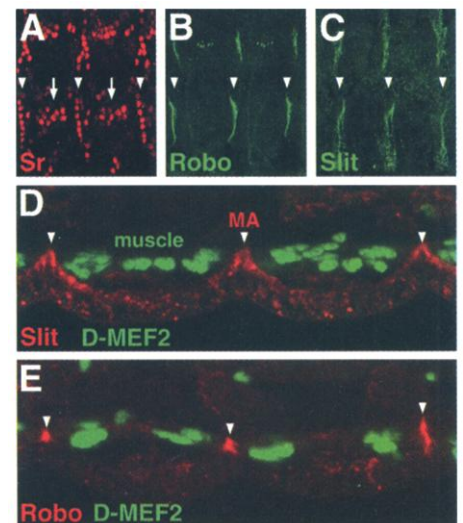
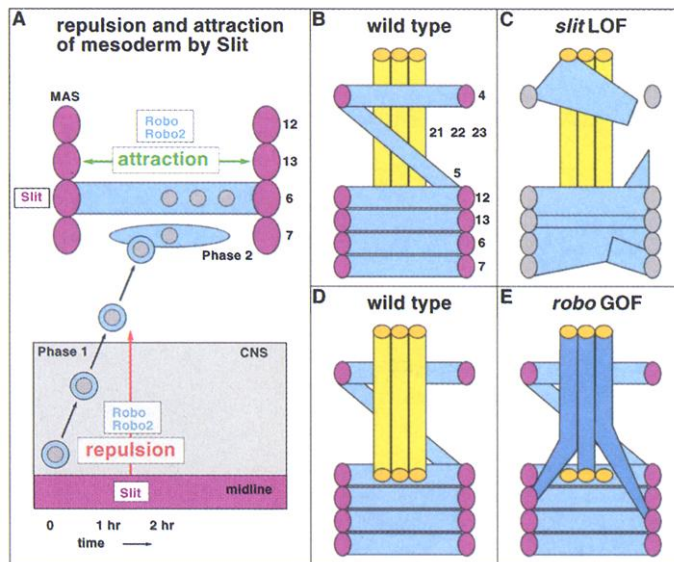


Fig. 2. Slit and Robo are coexpressed at a subset of MASs, as shown by confocal sections of stage 16 wild-type embryos labeled with antibody to Stripe (Sr) (red), antibody to Robo (green), or antibody to Slit (green). Dorsal is up, and anterior is to the left in each panel. (A) Sr is present in all MASs, including those for ventral longitudinal muscles 6, 7, 12, and 13 (arrowheads) and for lateral transverse muscles 21 through 23 (arrows). (B) Robo is expressed by the longitudinal muscles and is restricted to the sites of contact between the muscles and their MASs (arrowheads). Robo staining is absent in the transverse muscles [compare with arrows in (A)]. The dorsal segmentally repeated structures are the chordotonal organs. Robo2 has an identical expression pattern at this stage (27). (C) Slit is expressed by epidermal cells and localizes to a subset of MASs (arrowheads). Slit staining is absent from MASs for the lateral transverse muscles. Cross sections through the body wall of wild-type stage 16 embryos costained for (D) Slit or (E) Robo (red) and D-MEF2, which labels muscle nuclei (green). Slit localizes to the outer epidermal cell layer and is concentrated to the sites of muscle attachment (MA) (arrowheads), whereas Robo is concentrated at the ends of the muscles, where they make contacts with the epidermis at segment borders (arrowheads).

change in the muscle pattern (Fig. 4G). However, when endogenous *MAS slit* is removed at the same time, we observe dramatic muscle patterning defects. Dorsal muscles 1, 2, 9, and 10 normally stretch across from one segment border to another (11). These muscles, which express Robo receptors, stretch across the segment but often misattach in *slit* mutants (31). However,

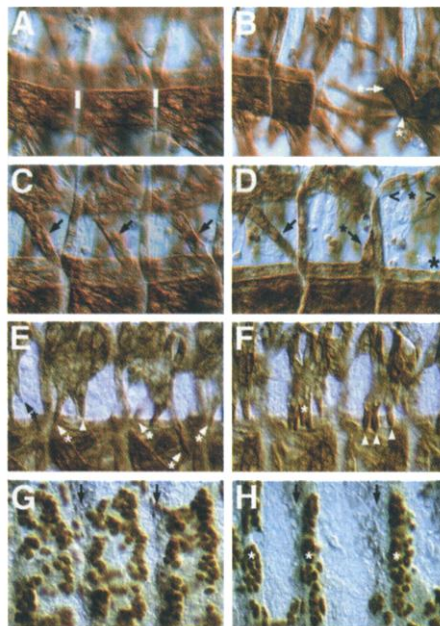
in *slit, en-GAL4; UAS-slit* embryos, these muscles frequently fail to stretch across each segment and instead align themselves along the stripe of ectopic Slit (Fig. 4H). Similar results are obtained with the *patched-GAL4* line (31). Thus, the expression of Slit in the epidermis is sufficient to provide an attractive cue to migrating mesoderm cells.

Fig. 3. Repulsion and attraction by Slit. (A) Schematic illustrating the bifunctional nature of Slit during two phases of myogenesis. During the first phase (bottom), Slit (pink) functions as a repellent at the midline for migrating mesoderm cells that express Robo and Robo2 (blue). Several hours later, these same cells, which continue to express the Robo receptors, are now attracted to MASs expressing Slit. (B and D) Wild-type muscle pattern showing the Robo-positive lateral muscles 4 through 7, 12, and 13 (blue), as well as the Robo-negative transverse muscles 21 through 23 (yellow). MASs expressing Slit are labeled in pink. Slit is absent from the MASs for muscles 21 through 23. (C) In *slit* loss-of-function (LOF) embryos, Robo-positive muscles are frequently found attached to the wrong sites in the epidermis. Muscles 21 through 23 remain largely unaffected. (E) Ectopic expression of Robo or Robo2 [gain of function (GOF)] in muscles 21 through 23 causes these muscles to turn and attach to sites that express high levels of Slit.



in *slit, en-GAL4; UAS-slit* embryos, these muscles frequently fail to stretch across each segment and instead align themselves along the stripe of ectopic Slit (Fig. 4H). Similar results are obtained with the *patched-GAL4* line (31). Thus, the expression of Slit in the epidermis is sufficient to provide an attractive cue to migrating mesoderm cells.

Fig. 4. Muscle guidance is dependent on Slit or Robo dosage (refer to Fig. 3 for muscle identification). Dorsal is up and anterior is to the left in each panel. Myosin staining is shown in (A and C) wild-type and (B and D) *slit, sim-GAL4; UAS-slit* embryos. As shown in (A), muscles 6 and 7 normally run parallel to each other. In *slit* embryos (B), these muscles do not reach their MASs (arrow with *) or make abnormal connections with the epidermis (arrowhead with *). As shown in (C), muscle 5 (arrows) normally stretches obliquely between muscle 4 and muscle 12. In *slit* embryos (D), this muscle is often missing (indicated by *) or not properly attached (arrow with *). Muscle 4 is also often not properly attached in these embryos (marked by <*>). (E) Myosin staining in a stage 16 embryo carrying one copy of *UAS-robo* and *24B-GAL4*. Here, 50% of lateral transverse muscles ($n = 71$) expressing ectopic Robo are attracted to the segment borders at sites that express high levels of Slit (indicated by arrowheads with *). Similar results were obtained with *UAS-robo2*. (F) In *slit; UAS-robo/24B-GAL4* embryos, these muscles make normal attachments in 98% of segments counted ($n = 104$) (arrowheads). As typical for *slit* mutants, we occasionally detect an extra transverse muscle (marked by *). (G) Ectopic expression of Slit in a pattern of Engrailed stripes in a wild-type background results in little change in the overall muscle pattern as visualized by staining with antibody to D-MEF2, which stains the muscle nuclei. (H) The muscle pattern is dramatically altered by simultaneous removal of endogenous *slit* and ectopic expression of Slit in Engrailed stripes. The muscle cells now align with the stripes of ectopic Slit (marked by *). Ectopic Slit is stained blue and is slightly out of the plane of focus (arrows).



The data presented here lead to four conclusions. First, Slit is a bifunctional guidance cue in vivo. It has been shown that, in addition to its role as a repellent, Slit can function as a branch-inducing factor in vitro (32). Here we show that for migrating mesoderm cells in vivo, Slit functions as a chemorepellent at the midline and as a chemoattractant at MASs (Fig. 3A). Second, members of the Robo receptor family are required for both functions. At present, we do not know whether this conversion from repulsion to attraction reflects a change in another receptor subunit or a change in the internal state of the cell. Third, individual cells in vivo switch their response to Slit from repulsion to attraction. For ventral muscles 6 and 7 precursors, Slit is repulsive during the first phase of their migration away from the midline and then attractive during the second phase of their migration toward their specific MASs. This switch in responsiveness takes place within a few hours (Fig. 3A). Fourth, to our knowledge, Slit provides the first example of a guidance molecule shown to provide specificity for muscle patterning. In the absence of Slit, certain muscles lose their way. Moreover, when the Slit receptors Robo or Robo2 are ectopically expressed in muscles that normally do not express them, these muscles incorrectly extend toward Slit-expressing MASs.

How do cells in vivo convert their responsiveness over only a few hours? In vitro, changing the levels of cyclic nucleotides can convert attraction to repulsion and vice versa (9, 10). With an in vivo model for switching, it will be of interest to determine the molecular mechanism whereby cells in a developing organism switch their responsiveness from repulsion to attraction.

References and Notes

1. M. Tessier-Lavigne, C. S. Goodman, *Science* **274**, 1123 (1996).
2. J. T. W. Wong, W. T. C. Yu, T. P. O'Connor, *Development* **124**, 3597 (1997).
3. D. Bagnard, M. Lohrum, D. Uziel, A. W. Püschel, J. Bolz, *Development* **125**, 5043 (1998).
4. D. Van Vactor, J. C. Flanagan, *Neuron* **22**, 649 (1999).
5. F. Polleux, T. Morrow, A. Ghosh, *Nature* **404**, 567 (2000).
6. R. Shirasaki, R. Katsumata, F. Murakami, *Science* **279**, 105 (1998).
7. T. Kidd *et al.*, *Cell* **92**, 205 (1998).
8. M. Su *et al.*, *Development* **127**, 585 (2000).
9. G. L. Ming *et al.*, *Neuron* **19**, 1225 (1997).
10. H. Song *et al.*, *Science* **281**, 1515 (1998).
11. M. K. Baylies, M. Bate, M. Ruiz Gomez, *Cell* **93**, 921 (1998).
12. This process was first described in another insect [R. K. Ho, E. E. Ball, C. S. Goodman, *Nature* **301**, 66 (1983)].
13. T. Volk, *Trends Genet.* **15**, 448 (1999).
14. J. M. Rothberg, J. R. Jacobs, C. S. Goodman, S. Artavanis-Tsakonas, *Genes Dev.* **4**, 2169 (1990).
15. T. Kidd, K. S. Bland, C. S. Goodman, *Cell* **96**, 785 (1999).
16. See Web table 1 in supplemental material (33).
17. See Web fig. 1 in supplemental material (33).
18. See "Genetic stocks and reagents" in supplemental material (33).
19. K. Brose *et al.*, *Cell* **96**, 795 (1999).

20. J. H. Simpson, T. Kidd, K. S. Bland, C. S. Goodman, *Neuron* **28**, 753 (2000).
21. J. H. Simpson, K. S. Bland, R. D. Fetter, C. S. Goodman, *Cell* **103**, 1019 (2000).
22. S. Rajagopalan, E. Nicolas, V. Vivancos, J. Berger, B. J. Dickson, *Neuron* **28**, 767 (2000).
23. S. Rajagopalan, V. Vivancos, E. Nicolas, B. J. Dickson, *Cell* **103**, 1033 (2000).
24. M. Ruiz-Gomez, N. Coutts, A. Price, M. V. Taylor, M. Bate, *Cell* **102**, 189 (2000).
25. S. Becker, G. Pasca, D. Strumpf, L. Min, T. Volk, *Development* **124**, 2615 (1997).
26. B. Lilly *et al.*, *Science* **267**, 688 (1995).
27. S. G. Kramer, C. S. Goodman, unpublished data.
28. See Web fig. 2 in supplemental material (33).
29. C. A. Callahan, J. L. Bonkovsky, A. L. Scully, J. B. Thomas, *Development* **122**, 2761 (1996).
30. See Web fig. 3 in supplemental material (33).
31. See "Slit gain of function" in supplemental material (33).
32. K. H. Wang *et al.*, *Cell* **96**, 771 (1999).
33. Supplemental material is available at www.sciencemag.org/cgi/content/full/292/5517/737/DC1.
34. We thank S. Carroll, M. Frasch, B. Patterson, T. Volk, and G. Vorbrüggen for fly stocks and antibodies and D. Parnas, G. Bashaw, M. Poo, J. Thomas, and N. Brown for comments and helpful discussions. S.G.K. was supported by a grant from the Spinal Cord Research Foundation, and C.S.G. was supported by NIH grant NS18366 and Christopher Reeve Paralysis Foundation grant GBC1-9801-2. C.S.G. is an Investigator and J.H.S. is a Predoctoral Fellow with the Howard Hughes Medical Institute.

3 January 2001; accepted 30 March 2001

Differentiation of Embryonic Stem Cell Lines Generated from Adult Somatic Cells by Nuclear Transfer

Teruhiko Wakayama,^{1*†} Viviane Tabar,² Ivan Rodriguez,¹ Anthony C. F. Perry,^{1*} Lorenz Studer,^{2†} Peter Mombaerts¹

Embryonic stem (ES) cells are fully pluripotent in that they can differentiate into all cell types, including gametes. We have derived 35 ES cell lines via nuclear transfer (ntES cell lines) from adult mouse somatic cells of inbred, hybrid, and mutant strains. ntES cells contributed to an extensive variety of cell types, including dopaminergic and serotonergic neurons in vitro and germ cells in vivo. Cloning by transfer of ntES cell nuclei could result in normal development of fertile adults. These studies demonstrate the full pluripotency of ntES cells.

Stem cells are able to differentiate into multiple cell types, representatives of which might be harnessed for tissue repair in degenerative disorders such as diabetes and Parkinson's disease (1). One obstacle to therapeutic applications is obtaining stem cells for a given patient. A solution would be to derive stem cells from embryos generated by cloning from the nuclei of the individual's somatic cells. We have previously cloned mice by microinjection using a variety of cell types as nucleus donors, including embryonic stem (ES) cells (2–4). We sought to perform the converse experiment by deriving ES cell lines in vitro from the inner cell mass (ICM) of blastocysts clonally produced by nuclear transfer.

To this end, nuclei from adult-derived somatic donor cells of five strains, including inbred (e.g., 129/Sv and C57BL/6^{mut/mut}, nude) and F₁ hybrid (e.g., C57BL/6 × DBA/2) representatives were transferred by microinjection (5) to produce cloned blastocysts (Table 1). When plated on fibroblast feeder layers in culture medium (6), cloned blastocysts from all five

strains tested yielded at least one nuclear transfer ES (ntES) cell line (Table 1) (8). Cultures were established from XX embryos derived via cumulus cell nuclear transfer (14.2% of blastocysts) and both XX and XY embryos derived from tail-tip cells (6.5%; Table 1). In total, 35 successfully cryopreserved stable ntES cell lines were produced.

Clonal origin of ntES cell lines was confirmed by polymerase chain reaction (PCR) analysis of polymorphic markers (8, 9). The ntES cell morphology of most lines was similar to that of widely disseminated lines such as E14 (11). We found no evidence for a pronounced difference in the efficiency of ntES cell line establishment between inbred and hybrid backgrounds (Table 1). All ntES cell lines tested expressed markers diagnostic for undifferentiated ES cells (12), including alkaline phosphatase (8) and Oct3/4 (13).

Embryonic stem cells have been induced to differentiate in vitro to produce cardiomyocytes (14), neurons (15), astrocytes and oligodendrocytes (16), and hematopoietic lineages (17). To assess the pluripotency of ntES cells, we therefore sought (i) to differentiate them in vitro to a wide variety of ectodermal, mesodermal, and endodermal lineages, and (ii) to induce a highly differentiated cell type. We chose a particularly specialized example with therapeutic potential: dopaminergic neurons.

Differentiation of embryoid bodies (8, 18) derived from three different ntES cell lines resulted in a mixed population of ectodermal, endodermal, and mesodermal derivatives (19). Efficient neural differentiation of ntES cells could be readily induced in each of the seven lines tested. Generation of specific midbrain dopaminergic neurons from ntES cells was achieved with a range of efficiencies by using a multistep differentiation protocol described previously (15, 20) (Fig. 1, A and B). One ntES cell line yielded dopaminergic neurons in excess of 50% of the total cell number. The functional nature of these neurons was confirmed by reversed-phase HPLC (RP-HPLC) determination of dopamine release (21) (Fig. 1C). Serotonergic neurons were also detected histochemically, although in smaller numbers, and serotonin release was confirmed by RP-HPLC (Fig. 1, D and E).

Two recent reports (22, 23) describe a total of five mouse ES cell-like lines derived from the ICMs of cloned blastocysts, although none contributed to the germ line. We characterized the contribution of 19 ntES cell lines to chimeric offspring after ntES cell injection into fertilization-derived blastocysts from the ICR strain (24). The contribution of ntES cells to 105 chimeric offspring after 348 blastocyst injections is summarized in Table 1. The contribution can be readily approximated by coat color, because all ntES cell lines are derived from black-eyed strains with dark coat color, whereas ICR is albino (Fig. 2, A and B). ntES cell lines generally contributed strongly to the coats of chimeric offspring (Table 1). This was corroborated for ntES cells derived from a hybrid strain ubiquitously expressing high levels of the reporter transgene, *EGFP* (25). All internal organs examined from two *EGFP* Tg chimeras contained an extensive contribution from the *EGFP*-expressing ntES cells (13).

As a comprehensive measure of pluripotency, the ability to contribute to the germ line is considered a defining characteristic of ES cells. Chimeric offspring were crossed with the albino strain, ICR. In ongoing experiments, 29 pups have been derived after chimera × ICR crosses as judged by eye and coat color and, where appropriate, *EGFP* expression (Table 1). Germ line transmission was demonstrated for seven ntES cell lines

¹The Rockefeller University, New York, NY 10021, USA. ²Laboratory of Stem Cell and Tumor Biology, Neurosurgery and Cellular Biochemistry and Biophysics, Sloan Kettering, New York, NY 10021, USA.

*Present address: Advanced Cell Technology, One Innovation Drive, Worcester, MA 01605, USA.

†To whom correspondence should be addressed. E-mail: teru@advancedcell.com; studerl@mskcc.org